RAA 2021 Vol. **21** No. **11**, 275(8pp) doi: 10.1088/1674-4527/21/11/275

http://www.raa-journal.org *http://iopscience.iop.org/raa*

Research in Astronomy and Astrophysics

Fallback in bipolar planetary nebulae?

Willem A. Baan[1,2,3], Hiroshi Imai[2,4] and Gabor Orosz[2,3,5]

[1] Netherlands Institute for Radio Astronomy ASTRON, 79901 PD Dwingeloo, Netherlands; *baan@astron.nl*
[2] Center for General Education, Institute for Comprehensive Education, Kagoshima University, 1-21-30 Korimoto, Kagoshima 890-0065, Japan
[3] Xinjiang Astronomical Observatory, Urumqi 830011, China
[4] Amanogawa Galaxy Astronomy Research Center, Graduate School of Science and Engineering, Kagoshima University, 1-21-35 Korimoto, Kagoshima 890-0065, Japan
[5] School of Natural Sciences, University of Tasmania, Private Bag 37, Hobart, Tasmania 7001, Australia

Received 2021 April 26; accepted 2021 July 28

Abstract The subclass of bipolar Planetary Nebulae (PNe) exhibits well-defined low-power outflows and some shows shock-related equatorial spiderweb structures and hourglass structures surrounding these outflows. These structures are distinctly different from the phenomena associated with spherical and elliptical PNe and suggest a non-standard way to simultaneously energise both kinds of structures. This paper presents evidence from the published literature on bipolar PN Hb 12 and other sources in support of an alternative scenario for energising these structures by means of accretion from material shells deposited during earlier post-AGB and pre-PNe evolutionary stages. In addition to energising the bipolar outflow, a sub-Eddington accretion scenario could hydrodynamically explain the spiderweb and outer hourglass structures as oblique shockwaves for guiding the accreting material into the equatorial region of the source. Estimates of the accretion rate resulting from fallback-related spherical accretion could indeed help to drive a low-power outflow and contribute to the total luminosity of these sources.

Key words: ISM: planetary nebulae: general — ISM: planetary nebulae: individual Hb 12, Hen 2-104, MyCn 18 — ISM: jets and outflows — stars: evolution

1 INTRODUCTION

Planetary nebulae (PNe) represent the post-evolution stages of medium mass stars leaving the Asymptotic Giant Branch (AGB) before its stellar core eventually turns into a white dwarf (Balick & Frank 2002). At the end of AGB evolution a superwind depletes the AGB envelope until the stellar structure changes, the photospheric radius shrinks and the stellar effective temperature rises (De Marco 2009). The further evolution of PNe is then affected by the occurrence of multiple 'late and very-late thermal pulse cycles' at the stellar core (Balick & Frank 2002), the fallback of AGB shells (Perinotto et al. 2004; Chen et al. 2016), and the ionisation of surrounding material by the central star, which make the PN move back and forth across the Hertzsprung-Russell (HR) diagram (Werner & Herwig 2006). Radiation hydrodynamical modelling of AGB-to-PN evolution demonstrates how the central-star mass and the (post-)AGB mass-loss history determine the shape and the kinematics of the resulting PN (Perinotto et al. 2004; Schonberner et al. 2005).

The complexity of the evolutionary processes of PNe can provide for the wide variety in colour and shape of spherical and elliptical PNe. However, the existence of spherical shells and ionisation fronts does not explain any of the structures observed in bipolar PNe (Balick & Frank 2002). The small number of bipolar (elongated) PN structures indicates the existence of a directed outflow that has been described as a stellar wind emanating from the inner layers of the stellar structure and blowing out along the symmetry axis (Mellema & Frank 1995; Balick & Frank 2002). A few sources exhibit a well-defined 'hourglass' axisymmetric structure that defines the interaction boundaries of an expanding outflow with the surrounding circumstellar material (Sahai et al. 1999). Alternatively, bipolar sources have been associated with a companion star in order to create a systematic asymmetry or have been explained by accretion in a symbiotic binary system, as in the case of the Twin Jet Nebula (Corradi et al. 2011). One out of five PNe have indeed been confirmed to host a binary companion (Miszalski et al. 2015) but the evidence for a 'binary hypothesis' is not yet very strong as compared with the 'single star hypothesis' for PNe (De Marco 2009).

Two of the prominent hourglass sources, Hb 12 and MyCn 18, display a Spiderweb arc structure in the equatorial plane of the system (perpendicular to the hourglass) that has (following tradition) been explained by repeated stellar wind outflows (Clark et al. 2014; Sahai et al. 1999), by sequential ejections resulting from a thermal nuclear runaway (Kwok & Hsia 2007) or by episodes of activity during earlier evolutionary stages (Vaytet et al. 2009). However, there is no clear explanation for a simultaneous outflow along the polar axis and the structure in the equatorial plane. Similarly, intermittent jets or winds blown by an accreting binary system have also been invoked to explain both the inner arc structure of the Red Rectangle (HD 44179) and its (perpendicular) outer structure (Soker 2005; Bujarrabal et al. 2016). Since bipolar PNe do not show any ionised shells that are characteristic of evolved PNe, they seem to be either at a very early evolutionary stage or at the end of PN evolution. The suggestion has indeed been made for these to be low-excitation and young sources that only recently started ionising their surrounding shells and represent a short transition stage toward full development (Clark et al. 2014).

The evolution of a PN is known to be strongly affected by fallback by material deposited in the surrounding interstellar environment by AGB and PN evolutionary activity. However, no clear scenario has been established to recognise when fallback actually occurs. While fallback may happen unnoticed observationally when the accretion rate is very low and streams of fallback material may leak into the atmosphere of the central star of the PN, a definite accretion signature should be established when the accretion rate becomes high. When the accretion rate becomes higher because of the availability of accretion material, sub-Eddington accretion may happen where the low luminosity of the PN source cannot cause the accretion flow to stagnate. The power generated during this (possibly short-lived) accretion could still be sufficient to energise activity in the PN. Although existing explanations for bipolar PN sources have traditionally relied on nuclear activity of the source itself, an accretion scenario should also be considered to drive an outflow along the polar axis and also explain any structures close to the equatorial plane.

In this paper, we seek qualitative evidence from the published literature that would support the possibility of semi-spherical sub-Eddington accretion onto a bipolar source such as PN Hb 12. The origin of the accreting material may be the ejecta during earlier AGB stages that have been deposited in the surrounding medium of a post-AGB environment of a bipolar PN. Alternatively, accretion could also occur during or at the end of the PN evolutionary path with diminished/ceased stellar activity but the accretion rate from the interstellar medium (ISM) may not be sufficient during these stages. The evidence for an accretion scenario in a bipolar source such as PN Hb 12 will set the stage for further research on bipolar PNe. After describing the structural evidence of bipolar PN Hb 12 in Section 2, available observational evidence is presented in Section 3 that would directly support or be consistent with an accretion-outflow scenario.

2 THE BIPOLAR STRUCTURE OF PN HB 12

The bipolar Matryoshka Nebula PN Hb 12 has been very well studied and provides specific fundamental insights into the workings of a bipolar PN (Hora & Latter 1996; Welch et al. 1999; Kwok & Hsia 2007; Vaytet et al. 2009; Clark et al. 2014). Figure 1(left) presents a composite optical/infrared Hubble Space Telescope (HST) image of the central structure of Hb 12, which features hourglass-shaped 'bipolar outflow' channels seen in narrow band [N II] (λ 6584) observations (Balick 2003; Kwok & Hsia 2007). The axis of the hourglass outflow structure in PN Hb 12 with concentric ring structures in its boundary is tipped clockwise by 10° and with the upper part tilted away from the plane of the sky by 25° (Vaytet et al. 2009). In addition, prominent infrared [Fe II] (λ1.6435 μm) line emission displays the two edge section of an equatorial and axisymmetric Spiderweb structure together with the inner sections of a larger scale 'Outer Hourglass' structure (Clark et al. 2014). Figure 1(right) again shows the detailed [Fe II] equatorial Spiderweb structure surrounding the star and the continuation towards a bipolar Outer Hourglass structure that is less collimated than the (inner) outflow hourglass structure. This Outer Hourglass (shock) structure is expected to become less prominent with distance and will close beyond the stagnation point of the bipolar outflows; this closure has not yet been observed in Hb 12. The nearly face-on Hb 12 displays a very detailed east – west symmetry of the axisymmetric Spiderweb but also a north – south symmetry at either side. These structural details of the Spiderweb will be essential for understanding what is happening in these regions.

The bipolar outflow, the Spiderweb structure, and the outer hourglass structures found in Hb 12 and other bipolar sources are the defining structural components to be explained consistently in modelling these sources. Prominent co-axial structures emanating from the core

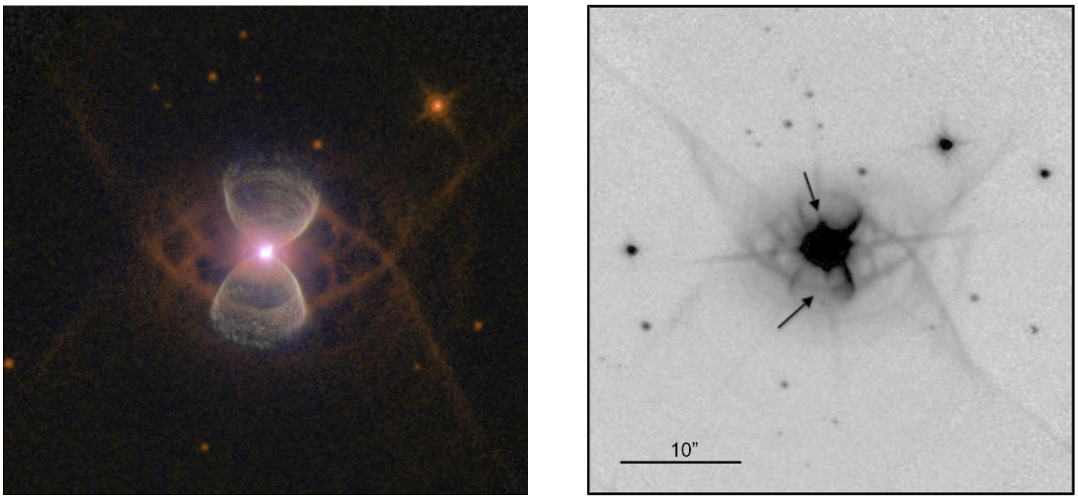

Fig. 1 (*Left*) A composite optical/infrared HST image displays the inner structure of the spatial structure of Matryoshka Nebula Hb 12 with the [N II](λ6584 µm) emission of the Spiderweb and the NICMOS F160W image featuring shocked [Fe II](λ1.6435 µm) emission from the boundary of the bipolar outflow. Photo: ESA/NASA/J. Schmidt. (*Right*) An HST NICMOS F160W image from the HST Legacy Archive depicting the detailed [Fe II] emission structures of the Spiderweb. The arrows point to the Spiderweb arcs detected in NICMOS F220W H_2 (λ2.1214 µm) data. The equatorial arcs are integrated with an outer and larger bipolar Hourglass structure. The field of view is $40'' \times 40''$. Image from Clark et al. (2014).

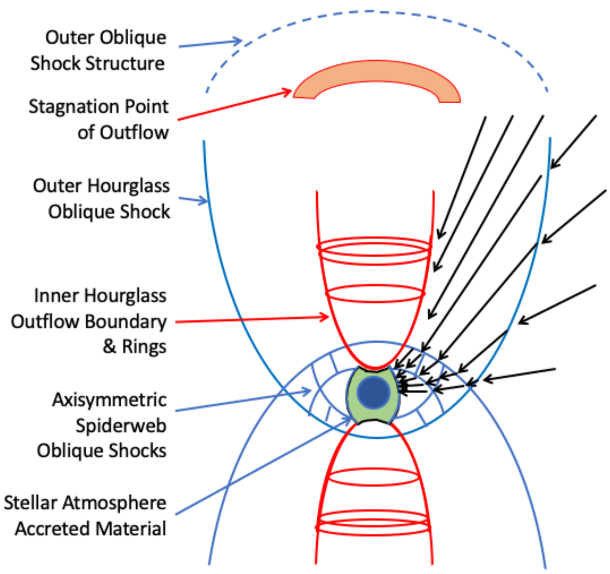

Fig. 2 Schematic of the structural components of PN Hb 12. The *red components* relate to the outflow patterns and the *blue components* relate to inflow patterns. The Inner Hourglass outflow boundary, and the Outer Hourglass and Spiderweb oblique shocks are clearly seen in the images of Hb 12 in Fig. 1. The *black arrows* in the upper right quadrant designate the accretion flow pattern through these (*blue*) oblique shock structures. A stagnation point of the (*red*) outflow in Hb 12 has also been observed at a significant distance of $75''$ from the star.

region are also found in the Hourglass Nebula PN MyCn 18 (Bryce et al. 1997), as well as in symbiotic bipolar nebulae such as the Southern Crab Hen 2-104, Menzel's young PN Ant Nebula Mz 3, Minkowski's Twin Jet (or Butterfly) Nebula M 2-9 (Corradi et al. 2001; Clyne et al. 2015, and references therein) and the post-AGB pre-PN (Rotten) Egg Nebula OH 231.8+04.2 (see Balick et al. 2020).

In this paper we adopt the distance to Hb 12 to be 2.24 kpc, which renders the $15''$ extent of these structures to be 0.16 pc (34 000 AU). In reality, the distances to Hb 12 (estimated to be from 2.24 to 14.25 kpc) and other PNe are highly uncertain, which makes size determinations difficult (Clark et al. 2014). Considering the extreme detail observed in the Spiderweb and the bipolar outflow in PN Hb 12, the distance could actually be less than the 2.24 kpc estimate. Further hydrodynamic modelling of the Spiderweb structures may facilitate a more accurate distance determination.

3 EVIDENCE FOR OUTFLOW AND INFLOW

The presence of outflows in bipolar PNe has been long recognised in the literature but the simultaneous occurrence of a bipolar outflow combined with Spiderweb and Outer Hourglass structures has not led to satisfactory explanations. In the following sections, we consider the existing literature for any evidence that accretion inflow may be driving the outflows in bipolar sources and that an accretion scenario consistently explains the nature of all observed structural components in Hb 12.

3.1 A Semi-Spherical Accretion and Outflow Scenario

The outflow structure, the Spiderweb and the outer structures observed in Hb 12 are delineated by forbidden [N II] (λ6584) and infrared [Fe II] (λ1.6435 µm) line emissions that all may be assumed to be related to shock heating and excitation. While the line emission associated with the outflow may be easily understood, the other line emission structures would suggest a non-outflow explanation. The existence of an accretion inflow close to the stellar surface would naturally result in an axisymmetric system of oblique shocks that guides the initially radial accretion inflow into the equatorial region and around the outflow structure as captured in the diagram of Figure 2. Hydrodynamically, an oblique shock stands under an angle with the flow direction and will thermalise part of the flow velocity component perpendicular to the shock, while leaving the parallel velocity component intact. Assuming that the underlying star has ceased its own shell burning activity and has no substantial stellar wind, the oblique shocks of the Outer Hourglass serve to decelerate and redirect the in-falling gas at large distances in order to guide the flow around the bipolar outflow regions and into the axisymmetric oblique shocks of the Spiderweb structure in the equatorial region. The very structured shock patterns observed around PN Hb 12 and other sources may thus be consistent with a hydrodynamic inflow pattern resulting from accretion, either spherical or from a distant companion star. While full hydrodynamical modelling of this inflow-outflow structure will be needed to further confirm this scenario, it will also provide a measure of the accretion rate, the strength of the oblique shocks and the actual scale size of the shock patterns (and indirectly the distance).

3.2 Bipolar Outflow in the Inner Hourglass

The bipolar Inner Hourglass outflow structure in Hb 12 represents a prominent feature in the source with the base seen in forbidden [Fe II] line emission and the outline of the whole structure seen in the lower density tracing forbidden [N II] emission (Fig. 1). The observed structure clearly suggests a low power outflow expanding into a pressure gradient and energising a widening boundary layer as outlined by the [Fe II] and [N II] line emission (Kwok & Hsia 2007; Vaytet et al. 2009). The shape of the boundary of this hourglass outflow channel suggests consistency with a supersonic and accelerating fluid outflow from a simple DeLaval-like nozzle expanding into a circumstellar medium with a radial pressure profile $p(r) \propto r^{-2}$ (using the formalism from Landau & Lifshits 1959; Choudhuri 1998). The boundaries of this outflow are self-adjusting and are determined by the equilibrium between the internal pressure of the accelerating flow and the radially varying ambient pressure in the circumstellar envelope. The supersonic outflow along the polar axis starts at a narrowed throat formed in the atmosphere where the gas reaches a proton escape velocity equaling the local velocity of sound. If the 90 km s^{-1}base velocity is indicative of the local escape velocity from a 1 $M_\odot$ star, then this Mach nozzle may form at a radius of about 10^{12} cm and require a local temperature of 10^5 K, which is higher than the effective surface temperature of 35 000 K (Hyung & Aller 1996). Our first order modelling of the case with a quadratic pressure gradient affirms that the flow accelerates early in the nozzle and may reach a final velocity of at least 2.5 times the sound velocity at the throat of the nozzle. Sustained operation of the nozzle outflow would require sustained replenishment of heated atmospheric material. Detailed modelling may provide an estimate of the power and the scale size of the outflow.

The boundary layer observed in Hb 12 and other sources will naturally develop around the outflow where the edges of the flow pattern are slowly decelerating because of energy and momentum being dissipated. This boundary layer of Hb 12 is very prominent with shock-tracer [Fe II] emission lines at the onset of the outflow and is seen in [N II] emission away from the star as the interaction becomes less intense (Clark et al. 2014). The velocities at the base of the Hb 12 outflow are estimated to be 90 $\pm$15 km s^{-1}in the redshifted (north) and blueshifted (south) senses and consistent with the velocity estimate mentioned above. Similar bipolar structures and outflow velocities have been detected in the PNe MyCn 18 (V = $\pm$48 km s^{-1}) (Corradi & Schwarz 1993), in Mz 3 (V = 130 km s^{-1}) (Santander-García et al. 2004) and the Inner Hourglass structure of the symbiotic Mira Hen 2-104 (V = 50 km s^{-1}) (Corradi et al. 2001; Clyne et al. 2015).

At a certain distance from the central star, bipolar outflows are expected to stagnate and produce lobes containing accumulated outflow and entrained material that are analogous to the radio lobes of extragalactic sources. The stagnation lobes in the low-power outflow of PN Hb 12 appear as multiple knots at a distance of 75″ (0.84 pc if at 2.24 kpc) that are emitting low-ionisation [N II] line emission (Vaytet et al. 2009). The velocities of these knots are at +275 (north) and −296 km s^{-1}, which are slightly higher than a few times the base velocity 90 km s^{-1}. Stagnation points have also been identified in the sources Hen 2-104 and the Rotten Egg Nebula (Corradi et al. 2001; Kwok & Hsia 2007).

The multiple coaxial rings in the walls of the hourglass outflow structures of Hb 12 are also seen as low-ionisation [N II] thermal emission (Kwok & Hsia 2007) and would result from energy dissipation in the boundary layer (see Fig. 1). These rings appear roughly equally spaced at approximately 850 AU (if at 2.24 kpc) and may result from some axisymmetric Kelvin-Helmholtz-like instability resulting from the velocity gradients across the boundary layer. Alternatively, these rings could represent decelerating shocks only in the boundary layer as a result of the decreasing ambient pressure shaping the outflow. Similar rings are also prominent in the sources MyCn 18 (Sahai et al. 1999), M 2-9 (Kwok & Hsia 2007) and Hen 2-104 (Corradi et al. 2001).

3.3 Evidence for Inflow at the Outer Hourglass

The Outer Hourglass oblique shock structure appears as two axisymmetric elliptical surfaces that reach around the star and interconnect with the Inner Spiderweb at its outer edge (see Fig. 2). In PN Hb 12 only the base of the shock-related [Fe II] Outer Hourglass emission structures can be seen in (Fig. 1) but they are expected to extend towards the stagnation points in the outflows (Vaytet et al. 2009). The axisymmetric region between the boundary layer of the Inner Hourglass outflow and the Outer Hourglass shocks would also be filled with in-falling material that has been shock-heated and may show H_2 and [N II] tracer emission. All shock-related [N II] and H_2 emissions within the Outer Hourglass structure are expected to decrease in intensity away from the star because of decreasing densities and decreasing perpendicular velocities in the oblique shocks. While Hb 12 does not (yet) exhibit such emissions, the filamentary [N II] λ6583 emitting cloudlets in PN Hen 2-104 trace a very similar Outer Hourglass structure far beyond the Inner Hourglass outflow (Corradi et al. 2001; Corradi 2003; Kwok & Hsia 2007). Similar emissions are found in the Twin Jet Nebula M 2-9 and PN Mz 3 (see Kwok & Hsia 2007; Clyne et al. 2015).

A long-slit velocity-position diagram taken along the major axis of the Hen 2-104 system demonstrates that the bipolar outflow has (accelerated) positive velocities in the north up to projected $+90\,\mathrm{km\,s^{-1}}$and negative velocities in the south (Corradi & Schwarz 1993; Corradi et al. 2001). However, the diagram also features opposite velocities in the north as well as in the south that increase up to projected velocities of $30\,\mathrm{km\,s^{-1}}$at the edge of the Outer Hourglass structure. While the bipolar Inner Hourglass shows an outflow pattern, the filaments inside the Outer Hourglass of Hen 2-104 would indeed represent the expected inflowing accretion component.

3.4 Inflow through the Spiderweb Structures

The apparent shock structures in both the equatorial Spiderweb and the Outer Hourglass structures are consistent with a large scale hydrodynamic flow pattern leading towards the stellar core in Hb 12. The series of oblique shocks redirect and decelerate the accretion flow, raise the density and the temperature, and funnel the flow into the equatorial region. The shock nature of these structures may be supported by the detection of the shock tracer [Fe II] (λ1.6436 µm) emission, continuum (λ1.6 µm) and the H_2 (λ2.1214 µm) line emission (Hora & Latter 1996; Clark et al. 2014). The two tangential edge sections of this axisymmetric system of standing oblique shocks elucidate in great detail how the inflow is being guided onto an equatorial surface of the star (Fig. 2). The nearly face-on position of Hb 12 also displays the north-south symmetry in the Spiderweb, which indicates that the flow pattern near the star is the same above and below the equatorial plane. Incidentally, these oblique shocks work on the same principles as a diffuser (air intake) of a supersonic airplane. The inner Spiderweb and the Outer Hourglass form an interconnected oblique shock network that takes the initially spherical accretion flow, bypasses the region of the bipolar outflow, and brings it into the equatorial region of the star.

Analysis of the molecular hydrogen emission in Hb 12 suggests that collisional processes would dominate over ultraviolet (UV) absorption for exciting the H_2 emission when the kinetic temperature $T_k > 1000\,\mathrm{K}$ (Hora & Latter 1996). The temperature of free-falling material at a distance R from a star would be considerably high at $T_{ff} = 1.08\times10^5\, M_\odot\, R_{AU}^{-1}$ K. This suggests that shock heating of the accreting material would completely dominate the excitation of H_2 inside a radius of about 100 AU from the star.

In addition to PN Hb 12, evidence for similar Spiderweb structures has been found in bipolar PNe such as MyCn 18 (Bryce et al. 1997), Henize 2-104 (Corradi et al. 2001; Clyne et al. 2015), R Aqr (Corradi & Schwarz 1995), Mz 3 and M 2-9 (Clyne et al. 2015).

3.5 Infall in the Vicinity of the Stellar Surface

A final standing shock must exist above the equatorial stellar surface in order to further decelerate the (then) nearly radial flow pattern to a subsonic velocity and to let this inflow integrate with the stellar atmosphere and a possible circumstellar disk. Existing observational data of the H_2 and [Fe II] emissions in Hb 12 taken just north of the core, at the core and just south of the core provide evidence for this inflow inside the Spiderweb of Hb 12 (fig. 2 in Clark et al. 2014). At the 'northern edge' of the nuclear region and covering the edge of the Inner Hourglass, the shock tracer [Fe II] emission features a redshifted northern outflow with a (projected) velocity in the range of $+30$ to $+60\,\mathrm{km\,s^{-1}}$. However, there are also positive velocities in the [Fe II] and H_2 data south of the core at the edge of the Spiderweb in the range 0 to $+30\,\mathrm{km\,s^{-1}}$. Similarly, the blueshifted 'southern' outflow is seen south of the core in the [Fe II] data at -60 to $-30\,\mathrm{km\,s^{-1}}$, while the H_2 data also show emission north of the core at the Spiderweb structure in the range -30 to $0\,\mathrm{km\,s^{-1}}$. While the strongly positive and negative velocity components in the [Fe II] data can be explained as being part of the bipolar outflow, the smaller velocity components in the same direction at opposite sides of the core do not fit the picture. A simple interpretation of these components would be that velocities in the same direction (positive or negative) at either (north and south) side of the tilted source indicate that one can represent an outflow and then the other is an inflow. This suggests that the observational data presented by Clark et al. (2014) represent an outflow-inflow velocity pattern that is consistent with an accretion scenario.

3.6 Evidence for a Disk around the Central Star

The accretion flow into an equatorial footprint may result in the formation of a thick disk/torus around the central star as a form of temporary mass storage before material transfers into the atmosphere of the star. Evidence for such an equatorial torus has indeed been found in Hb 12 using the bright He I (2.0585 µm) and Brγ (2.1655 µm) recombination line emission featuring a central cavity with a $0.2''\times0.41''$ (450×930 AU if at 2.24 kpc) inner torus structure (Clark et al. 2014). However, the observed velocity profile perpendicular to the symmetry axis indicates a rotation velocity of 90 $\mathrm{km\,s^{-1}}$, which would suggest an orbital radius in the disk of only 0.22 AU around one $M_\odot$ star (and an uncomfortable distance of only 2.2 pc to the observer).

The presence of a disk in a bipolar PN may also be confirmed by any maser activity to be detected at their central regions. OH (1665 MHz) and H_2O (22.12 GHz) maser features at the core region of the bipolar PN K 3-35 suggest a disk with an extent of 98 AU (if at 5 kpc) (Miranda et al. 2001). In addition, the OH and H_2O features at the core K 3-35 are redshifted relative to the OH (1667 MHz) maser components found in the bipolar outflows, which would further confirm inflow into the central region. OH and H_2O masers are also found in the core regions of other bipolar PNe (Gómez et al. 2008; Uscanga et al. 2014; Gómez et al. 2015). Similarly, the infalling SiO (43 GHz) masers in the bipolar post-AGB pre-PN (Rotten Egg) OH 231.8+04.2 have been interpreted as being part of a torus (Sánchez-Contreras et al. 2002).

The shock-heated material in the disk around the stellar core will contribute to emission of the source in addition to the ongoing or enhanced shell burning possibly triggered by the accreted material. The estimated effective surface temperature of Hb 12 is 35 000 K based on modelling of the observed emission lines (Hyung & Aller 1996), which suggests an early O-star classification and would indicate an early stage in PNe evolutionary models (Perinotto et al. 2004; Werner & Herwig 2006).

3.7 The Possibility of Sub-Eddington Accretion

Considering that bipolar PNe do not (yet) exhibit the shell-like characteristics of spherical and elliptical PNe, the possibility should be considered that the bipolar activity is driven by accretion in sources such as Hb 12. For early-type PNe the material may be accreted from a circumstellar cocoon/envelope or a large circumbinary disk that was formed during the later stages of post-AGB evolution (Perinotto et al. 2004; Herwig 2005; Akashi & Soker 2008). Simulations indicate that depending on the mass of the underlying star, such envelopes/shells may exist at distances ranging from a few to 10×10^{17} cm and have particle densities ranging from 20 to a few hundred $\mathrm{cm^{-3}}$ (Perinotto et al. 2004; Chen et al. 2016). During the early evolutionary PN phases lasting a few 10^4 yr, the free-fall timescale $t_{ff} = R^{3/2}/(2GM)^{-1/2}$ suggests that material within a radius of $R = 0.22\times10^{17}$ cm can fall back onto the star.

An accretion model that most adequately describes sub-Eddington accretion from a (distant) surrounding medium is the Bondi-Hoyle spherical accretion model (Bondi 1952; Mestel 1954). Because the luminosity of the source is not sufficient to halt the spherical accretion, the inflow is spherical until close to the stellar surface, where the polar outflow and the equatorial inflow regions compete for space. Assuming a uniform surrounding medium, a spherical accretion rate may be expressed for the temperature limited case with $\gamma = 3/2$ as (Bondi 1952) $\dot{M}_{\mathrm{acc}} = 2\pi\alpha(GM_{\mathrm{st}}^2(V^2 + c_s^2)^{-3/2}\rho_{\mathrm{ism}}) = 3.5\times10^{-9}M_{\mathrm{st}}^2\,n_{100}\,T_{10}^{-3/2}\,M_\odot\,\mathrm{yr^{-1}}$, where M_{st} is the stellar mass assumed to be 1 $M_\odot$, V is the spatial velocity of the star and is assumed to be zero, c_s is the speed of sound that depends on the temperature of the surrounding medium expressed in units of $T_{10} = 10\,\mathrm{K}$ and ρ_{ism} is the particle mass density of the medium far from the star expressed in units of $n_{100} = 100\,\mathrm{cm^{-3}}$. The factor α is between 1 and 2 depending on environmental conditions and a value of 1.5 is adopted here. The accretion rate favours higher stellar mass, higher gas densities and lower temperatures.

The luminosity resulting from the estimated accretion rate may be estimated as $L_{\rm acc} = \dot{M}_{\rm acc} G M_{\rm st}/R_{\rm st} = 2.9 \times 10^{33} M_1^3\, n_{100}\, T_{10}^{-3/2}\, R_{10}^{-1}\, {\rm erg\,s^{-1}}$, where the stellar radius $R_{\rm st}$ is expressed in units of 10^{10} cm.

An estimate of the luminosity of Hb 12 may follow from the estimated effective surface temperature of 35 000 K based on modelling of the observed emission lines (Hyung & Aller 1996), which results in a (minimum) blackbody luminosity for a stellar core with an effective radius 10^{11} cm to be $L_{\rm bb} = 8.8 \times 10^{36}\,{\rm erg\,s^{-1}}$. This value is less than the Eddington luminosity $L_{\rm Edd} = 1.2 \times 10^{38} M_1\,{\rm ergs^{-1}}$, which would verify that sub-Eddington accretion is possible for PN Hb 12. Assuming some reasonable parameters for the surrounding environment, a scenario with spherical accretion from fallback of circumstellar material could account for part of the apparent luminosity of the star and result in driving the outflow activity of Hb 12.

4 CONCLUSIONS

The presence of bipolar outflows seen in a subset of the PNe population may naturally result from accretion onto the star and the existing observational evidence of bipolar PN Hb 12 and similar sources would (already) support such a scenario. Published literature provides evidence that fallback of gaseous shells deposited during the earlier stages of post-AGB and pre-PN evolution may indeed provide sufficient material for sub-Eddington accretion. The shape of the boundaries of the low-power outflow in Hb 12 suggests that it is an accelerating and supersonic flow into an environment with a quadratic pressure gradient. A DeLaval-like nozzle may form in the stellar atmosphere where the gas reaches escape velocity equalling the sound speed from where the flow expands into the pressure gradient. The supplement of the accretion energy to the stellar atmosphere would be a trigger for establishing a bipolar outflow. The low luminosity of the stellar PN core is unable halt the accretion flow and establish an omni-directional stellar wind.

The unusual Spiderweb and Outer Hourglass structures observed in PN Hb 12 (and in similar sources) may be interpreted hydrodynamically as oblique shocks that decelerate the initially spherical accretion flow and redirect the flow pattern around the hemispherical sections of the bipolar outflows and into the equatorial region of the star. Evidence for infall follows from a detailed inspection of the imaging data of the [Fe II] and H_2 line emission of HB 12, where inflow velocity components are indeed co-located with outflow velocities in the core region. Similarly, the axisymmetric region between the Inner Hourglass boundary layer of the bipolar outflow and the oblique shocks of the Outer Hourglass would be filled with inflowing gas, as seen in emission in the similar Spiderweb source Hen 2-104. Also the presence of an accretion disk surrounding Hb 12 with a clear velocity gradient confirms that infalling material is collecting around the star. The estimate of the mass accretion rate using the Bondi-Hoyle model for spherical accretion shows that for reasonable parameters for the surrounding ISM environment, accretion of fallback shells could add significantly to the luminosity of the pre-PN source and provide enough energy to drive the bipolar outflows.

An episode with sub-Eddington accretion undoubtedly defines a separate evolutionary stage in the life of a PN. If the accreting material results from post-AGB activity, the star will acquire new material in its atmosphere, although some will be bipolar-ejected again and may fall back at a later time. After this accretion stage is finished, the star will initiate a further path of PN evolution with a new atmosphere. If this type of accretion happens during a later evolutionary stage of the PN, this will mark a temporary interruption of the PN activity to be followed by renewed PN activity with a replenished atmosphere. Since the availability of material to be accreted is an important factor, episodes of accretion depend very much on the details of AGB to PN and it is likely that stages of accretion will occupy only part of the evolutionary lifetime of a PN.

Further verification of the hydrodynamic interpretation of the accretion scenario will follow from (ongoing) modelling of the spherical Bondi-Hoyle accretion flow and the oblique shocks of the Spiderweb and the Outer Hourglass structures. Hydrodynamic modelling of the accretion flow and the supersonic DeLaval-nozzle bipolar outflow will provide an indication of the actual sizes of the oblique shock components and the outflow, and supply an independent estimate for the (uncertain) distance of these sources. Modelling efforts of the bipolar outflow and of the accretion flow have been initiated. A general verification of the accretion scenario would also result from (planned) radio observations of the shocks of the Spiderweb and the Outer Hourglass structure in Hb 12 and the (potential) detection of maser action in the shocked dense material of the disk in the system.

Acknowledgements WAB thanks the Graduate School of Science and Engineering of Kagoshima University and the Department of English Communication of Toyo University for their hospitality during the JSPS Invitation Program for Foreign Researchers (S15126). WAB also thanks Xinjiang Astronomical Observatory for their hospitality during the Program of High-end Foreign Experts of the Xinjiang Uygur Autonomous Region (Grant Nos. 20166500004 and 20176500001) and under the PIFI grant No. 2019VMA0040 from the Chinese Academy of Sciences. HI was supported by the JSPS KAKENHI program (JP16H02167). GO acknowledges support from the ARC Discovery project DP180101061 of the Australian Government, the CAS LCWR Program (2018-XBQNXZ-B-021) of China, the Japanese MEXT scholarship, the Leids Kerkhoven-Bosscha Fonds (LKBF17.0.002) and also thanks the support and hospitality of the Joint Institute for VLBI ERIC (JIVE).

Images made with the NASA/ESA Hubble Space Telescope are from the Hubble Legacy Archive, a collaboration between the Space Telescope Science Institute (STScI/NASA), the Space Telescope European Coordinating Facility (ST-ECF/ESA) and the Canadian Astronomy Data Centre (CADC/NRC/CSA).

References

Akashi, M., & Soker, N. 2008, New Astron., 13, 157

Balick, B. 2003, in Symbiotic Stars Probing Stellar Evolution, eds. R. L. M. Corradi, et al., ASP Conf. Ser., 303, 407

Balick, B., & Frank, A. 2002, ARA&A, 40, 439

Balick, B., Frank, A., Liu, B, & Huarte-Espinosa, M. 2020, ApJ, 843, 108

Bondi, H. 1952, MNRAS, 112, 195

Bryce, M., Lopez, J. A., Hollowat, A. J., & Meaburn, J. 1997, ApJL, 487, L161

Bujarrabal, V., Castro-Carrizo, A., Alcolea, M, Santander-Garcia, H., et al. 2016, A&A, 593, A92

Choudhuri, A. R. 1998, The physics of fluids and plasmas: an introduction for astrophysicist, (Cambridge: Cambridge Univ. Press)

Chen, Z., Frank, A., Blackman, E. G., & Nordhaus, J. 2016, MNRAS, 457, 3219

Clark, D. M., Lopez, J. A., Edwards, M. L., & Winge, C. 2014, AJ, 148, 98

Clyne, N., Akras, S., Steffen, W., Redman, M. P., et al. 2015, A&A, 582, A60

Corradi, R. L. M. 2003, in Symbiotic Stars Probing Stellar Evolution, eds. R. L. M. Corradi, et al., 303, 393

Corradi, R. L. M., & Schwarz, H. E. 1993, A&A, 268, 714

Corradi, R. L. M., & Schwarz, H. E., 1995, A&A, 293, 871

Corradi, R. L. M., Livio, M., Balick, B., et al. 2001, ApJ, 553, 211

Corradi, R. L. M., Balick, B., & Santander-García, M. 2011, A&A, 529, A43

De Marco, O., 2009, PASP, 121, 316

Gómez, J.F., Suárez, O., Gómez, Y., et al.. 2008, AJ, 135, 2074

Gómez, J., Suárez, O., Benjoya, P., et al. 2015, ApJ, 799, 186

Hyung, S., & Aller, L. H. 1996, MNRAS, 278, 551

Herwig, F. 2005, ARA&A, 43, 435

Hora, J. L., & Latter, W. B. 1996, ApJ, 461, 288

Kwok, S., & Hsia, C. H. 2007, ApJ, 660, 341

Landau, L. D., & Lifshitz, E. M. 1959, Fluid Mechanics (London: Pergamon Press)

Mellema, G., & Frank, A. 1995, MNRAS, 273, 401

Mestel, L. 1954, MNRAS, 114, 437

Miranda, L. F., Gómez, Y., Anglada, G., & Torrelles, J. M. 2001, Nature, 114, 284

Miszalski, B., Manick, R., & McBride, V. 2015, in The Physics of Evolved Stars: A Conference Dedicated to the Memory of Olivier Chesneau, eds. E. Lagadec, et al., EAS Publications Series, 71–72, 117

Perinotto, M., Schönberner, D., Stefffen, M., & Calonaci, C. 2004, A&A, 414, 993

Sahai, R., Dayal, A., Watson, A. M., et al. 1999, AJ, 118, 468

Sánchez-Contreras, C., Desmurs, J. F., Bujarrabal, V., et al. 2002, A&A, 385, 1

Santander-García, M., Corradi, R. L. M., Balick, B., & Mampaso, A. 2004, A&A, 426, 185

Schönberner, D., Jacob, R., Steffen, M., et al. 2005, A&A, 431, 963

Soker, N. 2005, AJ, 129, 947

Uscanga, L., Gómez, J. F., Miranda, L. F., et al. 2014, MNRAS, 444, 217

Vaytet, N. M. H., Rushton, A. P., Lloyd, M., et al. 2009, MNRAS, 398, 385

Welch, C. A., Frank, A., Pipher, J. L., et al. 1999, ApJL, 522, L69

Werner, K., & Herwig, F. 2006, PASP, 118, 183